Measurement of Atmospheric Neutrino Flux Consistent with Tau Neutrino Appearance

K. Abe,[1] Y. Hayato,[1] T. Iida,[1] K. Ishihara,[1] J. Kameda,[1] Y. Koshio,[1] A. Minamino,[1] C. Mitsuda,[1] M. Miura,[1] S. Moriyama,[1] M. Nakahata,[1] Y. Obayashi,[1] H. Ogawa,[1] M. Shiozawa,[1] Y. Suzuki,[1] A. Takeda,[1] Y. Takeuchi,[1] K. Ueshima,[1] I. Higuchi,[2] C. Ishihara,[2] M. Ishitsuka,[2] T. Kajita,[2] K. Kaneyuki,[2] G. Mitsuka,[2] S. Nakayama,[2] H. Nishino,[2] K. Okumura,[2] C. Saji,[2] Y. Takenaga,[2] Y. Totsuka,[2] S. Clark,[3] S. Desai,[3] F. Dufour,[3] E. Kearns,[3] S. Likhoded,[3] M. Litos,[3] J. L. Raaf,[3] J. L. Stone,[3] L. R. Sulak,[3] W. Wang,[3] M. Goldhaber,[4] D. Casper,[5] J. P. Cravens,[5] W. R. Kropp,[5] D. W. Liu,[5] S. Mine,[5] C. Regis,[5] M. B. Smy,[5] H. W. Sobel,[5] M. R. Vagins,[5] K. S. Ganezer,[6] J. E. Hill,[6] W. E. Keig,[6] J. S. Jang,[7] J. Y. Kim,[7] I. T. Lim,[7] K. Scholberg,[8] N. Tanimoto,[8] C. W. Walter,[8] R. Wendell,[8] R. W. Ellsworth,[9] S. Tasaka,[10] E. Guillian,[11] J. G. Learned,[11] S. Matsuno,[11] M. D. Messier,[12] A. K. Ichikawa,[13] T. Ishida,[13] T. Ishii,[13] T. Iwashita,[13] T. Kobayashi,[13] T. Nakadaira,[13] K. Nakamura,[13] K. Nitta,[13] Y. Oyama,[13] A. T. Suzuki,[14] M. Hasegawa,[15] I. Kato,[15] H. Maesaka,[15] T. Nakaya,[15] K. Nishikawa,[15] T. Sasaki,[15] H. Sato,[15] S. Yamamoto,[15] M. Yokoyama,[15] T. J. Haines,[16] S. Dazeley,[17] S. Hatakeyama,[17] R. Svoboda,[17] G. W. Sullivan,[18] A. Habig,[19] R. Gran,[19] Y. Fukuda,[20] T. Sato,[20] Y. Itow,[21] T. Koike,[21] C. K. Jung,[22] T. Kato,[22] K. Kobayashi,[22] M. Malek,[22] C. McGrew,[22] A. Sarrat,[1,22] R. Terri,[22] C. Yanagisawa,[22] N. Tamura,[23] M. Sakuda,[24] M. Sugihara,[24] Y. Kuno,[25] M. Yoshida,[25] S. B. Kim,[26] J. Yoo,[26] T. Ishizuka,[27] H. Okazawa,[28] Y. Choi,[29] H. K. Seo,[29] Y. Gando,[30] T. Hasegawa,[30] K. Inoue,[30] H. Ishii,[31] K. Nishijima,[31] H. Ishino,[32] Y. Watanabe,[32] M. Koshiba,[33] D. Kielczewska,[34,5] J. Zalipska,[34] H. G. Berns,[35] K. K. Shiraishi,[35] K. Washburn,[35] and R. J. Wilkes[35]

(Super-Kamiokande Collaboration)

[1]*Kamioka Observatory, Institute for Cosmic Ray Research, University of Tokyo, Kamioka, Gifu 506-1205, Japan*
[2]*Research Center for Cosmic Neutrinos, Institute for Cosmic Ray Research, University of Tokyo, Kashiwa, Chiba 277-8582, Japan*
[3]*Department of Physics, Boston University, Boston, Massachusetts 02215, USA*
[4]*Physics Department, Brookhaven National Laboratory, Upton, New York 11973, USA*
[5]*Department of Physics and Astronomy, University of California, Irvine, Irvine, California 92697-4575, USA*
[6]*Department of Physics, California State University, Dominguez Hills, Carson, California 90747, USA*
[7]*Department of Physics, Chonnam National University, Kwangju 500-757, Korea*
[8]*Department of Physics, Duke University, Durham, North Carolina 27708, USA*
[9]*Department of Physics, George Mason University, Fairfax, Virginia 22030, USA*
[10]*Department of Physics, Gifu University, Gifu, Gifu 501-1193, Japan*
[11]*Department of Physics and Astronomy, University of Hawaii, Honolulu, Hawaii 96822, USA*
[12]*Department of Physics, Indiana University, Bloomington, Indiana 47405-7105, USA*
[13]*High Energy Accelerator Research Organization (KEK), Tsukuba, Ibaraki 305-0801, Japan*
[14]*Department of Physics, Kobe University, Kobe, Hyogo 657-8501, Japan*
[15]*Department of Physics, Kyoto University, Kyoto 606-8502, Japan*
[16]*Physics Division, P-23, Los Alamos National Laboratory, Los Alamos, New Mexico 87544, USA*
[17]*Department of Physics and Astronomy, Louisiana State University, Baton Rouge, Louisiana 70803, USA*
[18]*Department of Physics, University of Maryland, College Park, Maryland 20742, USA*
[19]*Department of Physics, University of Minnesota, Duluth, Minnesota 55812-2496, USA*
[20]*Department of Physics, Miyagi University of Education, Sendai, Miyagi 980-0845, Japan*
[21]*Solar-Terrestrial Environment Laboratory, Nagoya University, Nagoya, Aichi 464-8601, Japan*
[22]*Department of Physics and Astronomy, State University of New York, Stony Brook, New York 11794-3800, USA*
[23]*Department of Physics, Niigata University, Niigata, Niigata 950-2181, Japan*
[24]*Department of Physics, Okayama University, Okayama, Okayama 700-8530, Japan*
[25]*Department of Physics, Osaka University, Toyonaka, Osaka 560-0043, Japan*
[26]*Department of Physics, Seoul National University, Seoul 151-742, Korea*
[27]*Department of Systems Engineering, Shizuoka University, Hamamatsu, Shizuoka 432-8561, Japan*
[28]*Department of Informatics in Social Welfare, Shizuoka University of Welfare, Yaizu, Shizuoka 425-8611, Japan*
[29]*Department of Physics, Sungkyunkwan University, Suwon 440-746, Korea*
[30]*Research Center for Neutrino Science, Tohoku University, Sendai, Miyagi 980-8578, Japan*
[31]*Department of Physics, Tokai University, Hiratsuka, Kanagawa 259-1292, Japan*
[32]*Department of Physics, Tokyo Institute for Technology, Meguro, Tokyo 152-8551, Japan*
[33]*University of Tokyo, Tokyo 113-0033, Japan*
[34]*Institute of Experimental Physics, Warsaw University, 00-681 Warsaw, Poland*
[35]*Department of Physics, University of Washington, Seattle, Washington 98195-1560, USA*
(Received 25 July 2006; published 23 October 2006)

A search for the appearance of tau neutrinos from $\nu_\mu \leftrightarrow \nu_\tau$ oscillations in the atmospheric neutrinos has been performed using 1489.2 days of atmospheric neutrino data from the Super-Kamiokande-I experiment. A best fit tau neutrino appearance signal of $138 \pm 48(\text{stat})^{+15}_{-32}(\text{syst})$ events is obtained with an expectation of $78 \pm 26(\text{syst})$. The hypothesis of no tau neutrino appearance is disfavored by 2.4 sigma.

DOI: 10.1103/PhysRevLett.97.171801 PACS numbers: 14.60.Pq, 95.55.Vj, 95.85.Ry

Atmospheric neutrino oscillations have been observed by several experiments [1–5]; in particular, Super-Kamiokande (Super-K) has reported the first evidence for the sinusoidal signature of muon neutrino disappearance [6] and made measurements of the oscillation parameters [7]. The Super-K atmospheric neutrino data favor $\nu_\mu \leftrightarrow \nu_\tau$ oscillations and have excluded $\nu_\mu \leftrightarrow \nu_e$ [1] and pure $\nu_\mu \leftrightarrow \nu_{\text{sterile}}$ oscillations [8] as a dominant source of the deficit of muon neutrinos. All of these results rely largely on the disappearance of muon neutrinos from the atmospheric neutrino flux, with no explicit observation of the appearance of tau neutrinos and their charged-current (CC) weak interactions. In this Letter, we analyze the Super-K atmospheric neutrino data in an attempt to demonstrate the appearance of ν_τ interactions in the detector.

Detection of CC ν_τ interactions in the atmospheric neutrinos is challenging for two reasons. First, the neutrino energy threshold for tau lepton production is 3.5 GeV. The atmospheric neutrino flux above this energy is relatively low. Assuming two flavor maximal mixing of $\nu_\mu \leftrightarrow \nu_\tau$ with $\Delta m^2 = 2.4 \times 10^{-3}$ eV^2, approximately one CC ν_τ event is expected to occur in an atmospheric neutrino detector per kiloton year of exposure. This corresponds to an estimated total of 78 ν_τ events in the data sample presented. Second, the tau lepton has a short lifetime (290 fs) and decays immediately into many different final states. These final states consist of electrons, muons, or one or more pions (plus always a tau neutrino). The recoiling hadronic system may also produce multiple particles. Water Cherenkov detectors such as Super-K are not suited for identifying individual CC ν_τ interactions as there are generally multiple Cherenkov rings with no easily identified leading lepton. Thus, we employ likelihood and neural network techniques to discriminate tau neutrino events from atmospheric neutrino events on a statistical basis.

Super-Kamiokande is a 50-kton water Cherenkov detector, with a rock overburden of 2700 m water equivalent, located in the Kamioka, Gifu prefecture in Japan. The detector consists of two concentric optically separated detector regions; the inner detector (ID) instrumented with 11 146 inward facing 20 in. diameter photomultiplier tubes (PMTs) and the outer detector (OD) instrumented with 1885 outward facing 8 in. PMTs. The details of the detector, calibrations, data reduction, and detector simulation can be found in Refs. [7,9].

In this Letter, the atmospheric neutrino data accumulated during the Super-K-I period (1489.2 live-day exposure) are analyzed. The atmospheric neutrino events in Super-K are classified as fully contained (FC), partially contained (PC), and upward-going muon events [7]. In the present analysis, only FC events are used. FC events deposit all of their Cherenkov light inside the ID, from which the direction and the momentum of charged particles are reconstructed. The particle type is identified as "e-like (showering)" or "μ-like (nonshowering)" for each Cherenkov ring based on the light-pattern [7].

Both tau neutrino and atmospheric neutrino (ν_e and ν_μ) interactions in Super-K are modeled using a Monte Carlo (MC) simulation, NEUT [7,10]. In our ν_τ MC simulation, only CC ν_τ interactions are simulated. CC ν_τ interactions are mostly deep-inelastic scattering (DIS) (approximately 63%) due to the high energy threshold for tau lepton production. The decays of tau leptons are simulated by the tau decay library, TAUOLA (version 2.6) [11]. The polarization of tau leptons produced via CC ν_τ interactions is also implemented from calculations by Hagiwara *et al.* [12].

The event signatures of tau neutrinos are characterized by the decays of tau leptons produced in CC ν_τ interactions. In this analysis, we concentrate on the hadronic decays of tau leptons (approximately 65% of tau lepton decays). The shape of events containing the hadronic decays of tau leptons has a more spherical topology than that of backgrounds. Also, the extra pions produced in tau lepton decays can be tagged by looking for their decays and ring signatures in the Super-K detector. The primary backgrounds for ν_τ signals are atmospheric neutrinos producing multiple pions via deep-inelastic scattering interactions. The following ν_τ event selection criteria are applied to reduce the backgrounds: (1) The vertex must be reconstructed in the fiducial volume (2 m from the ID PMT surface) with no activity in the OD region. (2) Visible energy (E_{vis}) must be greater than 1.33 GeV. (3) The most energetic ring must be e-like. These criteria can reduce the backgrounds by approximately 90% since the neutrino energy threshold in CC ν_τ interactions is higher than in most of atmospheric neutrino interactions and tau lepton decays have a high average multiplicity (resulting primarily in hadronic shower, i.e., e-like events). The effects of the event selection criteria are summarized in the first 3 lines of Table I.

In accordance with the event shape and characteristics of tau lepton decays, we define a set of five variables to further discriminate ν_τ signals from backgrounds, which are (a) visible energy, (b) maximum distance between the primary interaction and electron vertices from pion and then muon decays, (c) number of ring candidates,

TABLE I. Summary for the numbers of events in data, atmospheric neutrino ($\nu_{e,\mu}$) background MC events, and tau neutrino MC events after applying each of ν_τ event selection criteria and either the likelihood or the neural network cut, which is applied separately for each analysis. Neutrino oscillation is considered in the MC simulations with the oscillation parameters $\Delta m^2 = 2.4 \times 10^{-3}$ eV^2 and $\sin^2 2\theta = 1.0$, and the numbers are normalized by the live time of the data sample.

	Data	$\nu_{e,\mu}$ background MC events	CC ν_τ MC events
Generated in fiducial volume		17135 (100%)	78.4 (100%)
$E_{\rm vis} > 1.33$ GeV	2888	2943 (17.2%)	51.5 (65.7%)
Most energetic ring e-like	1803	1765 (10.3%)	47.1 (60.1%)
Likelihood > 0	649	647 (3.8%)	33.8 (43.1%)
NN output > 0.5	603	577 (3.4%)	30.6 (39.0%)

(d) sphericity in the laboratory frame, and (e) clustered sphericity in the center of mass frame (Fig. 1). The first two variables are Super-K standard variables [7]. The number of ring candidates is determined with a ring-finding algorithm, which is sensitive to ring fragments, and the last two variables, sphericity and clustered sphericity, are derived from a jet-based energy flow analysis.

The energy flow analysis uses Cherenkov patterns to deconvolve the measured light distribution in Super-K. By associating the deconvoluted power spectrum with pseudo particles, ''jets'' are reconstructed, and event shape variables such as sphericity are obtained. Sphericity ($0 < S < 1$) measures the spherical symmetry of an event and has a quadratic momentum dependence giving more weight to higher momentum particles [13,14]. Also, it is not invariant under the Lorentz transformation. Therefore, the sphericity calculated with different clustering and reference frames probes different event characteristics.

The expected distributions of each variable after applying the ν_τ event selection criteria for both signals and backgrounds are plotted in Fig. 1. The background MC events are compared with downward-going data, where no ν_τ appearance signal is expected, as the probability for ν_μ oscillating into ν_τ is very small for the given path length and the measured atmospheric Δm^2. The agreement of the downward-going data and background MC events indicates the variables chosen for this analysis are well modeled by our MC simulation. The small discrepancy in log (Sphericity) between the data and the atmospheric neutrino MC events is consistent with the systematic uncertainty in the vertex position.

We have constructed a likelihood function using the five variables described above. The data sample is divided into 5 energy bins: (1) $E_{\rm vis} < 2.0$, (2) $2.0 \leq E_{\rm vis} < 3.0$, (3) $3.0 \leq E_{\rm vis} < 6.0$, (4) $6.0 \leq E_{\rm vis} < 12.0$, (5) $12.0 \leq E_{\rm vis}$ [GeV]. The likelihood distributions for downward-going and upward-going events are shown in Fig. 2. The events for likelihood $\mathcal{L} > 0$ are defined to be taulike. The likelihood distributions of data and background MC events agree for downward-going events. The agreement validates our analysis method. Table I summarizes the number of data, atmospheric neutrino background MC events, and tau neutrino MC events after applying all of the event selection criteria.

A neural network (NN) is also trained with the five variables. The network has 6 input neurons, 10 hidden neurons, and one sigmoid output neuron and is trained using backpropagation by use of the MLPFIT neural network package [15]. The distributions of the NN outputs are shown in Fig. 2. NN output > 0.5 is defined to be taulike. The discrepancy between the data and MC just below the NN cut (NN output $= 0.5$) is consistent with the systematic uncertainty in the deep-inelastic scattering cross sec-

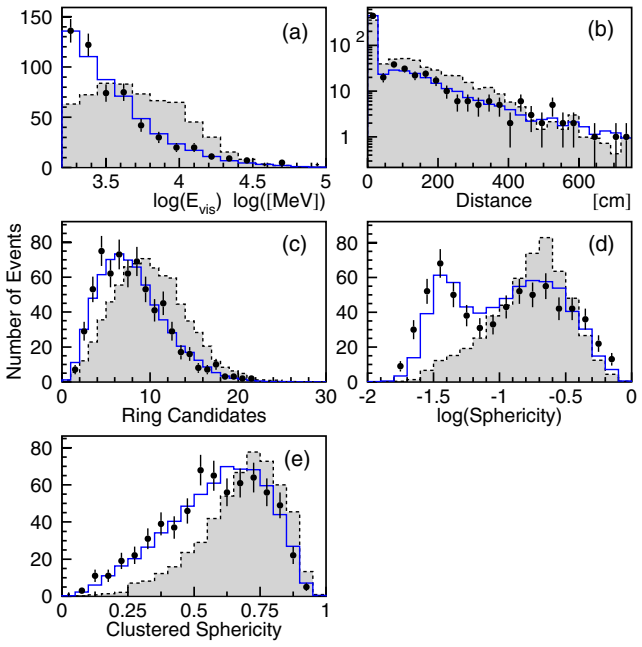

FIG. 1 (color online). The distributions of variables: (a) Visible energy, (b) maximum distance between the primary interaction and electron vertices from pions and then μ decays, (c) number of ring candidates, (d) sphericity in the laboratory frame, and (e) clustered sphericity in the center of mass, after applying the ν_τ event selection criteria for downward-going data (points), ν_τ MC events (shaded histogram), and atmospheric $\nu_{e,\mu}$ background MC events (solid histogram). (The histograms of ν_τ MC events are normalized arbitrarily.) In the likelihood analysis, the data sample is divided into 5 energy bins.

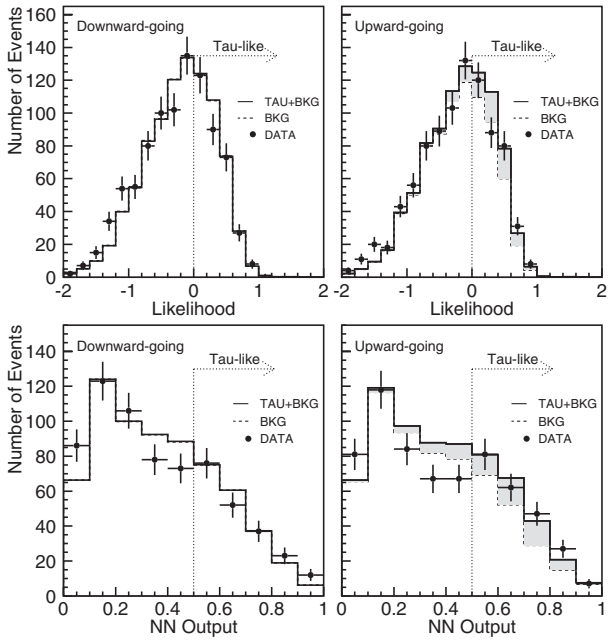

FIG. 2. The likelihood (top) and NN output (bottom) distributions of downward-going (left) and upward-going (right) events for data (points), atmospheric neutrino background (BKG) MC events (dashed histogram), and the best fit including tau neutrino and backgrounds (solid histogram). The shaded area shows a fitted excess of tau neutrino events in the upward-going direction. The events for likelihood $\mathcal{L} > 0$ or NN output > 0.5 are defined to be taulike.

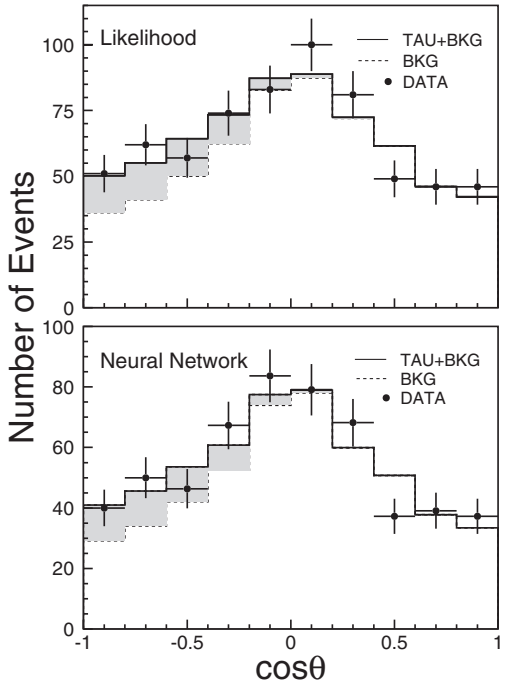

FIG. 3. The zenith angle distributions for the likelihood (top) and neural network (bottom) analyses. Zenith angle $\cos\theta = -1$ ($\cos\theta = +1$) indicates upward-going (downward-going) direction. The data sample is fitted after ν_τ event selection criteria are applied. The solid histogram shows the best fit including ν_τ, and the dashed histogram shows the backgrounds from atmospheric neutrinos (ν_e and ν_μ). A fitted excess of taulike events in the upward-going direction is shown in the shaded area.

tion near the threshold, which is included in the overall systematic uncertainty estimation described below.

After selecting the tau-enriched sample by applying the ν_τ event selection criteria with either the likelihood ($\mathcal{L} > 0$) or the neural network (NN output > 0.5) cut, the zenith angle distribution is fitted with a combination of the expected tau neutrino signals resulting from oscillations and the predicted atmospheric neutrino background events including oscillations. The fitted zenith angle distribution and the χ^2, which is minimized, are

$$N_{\text{total}}(\cos\theta) = \alpha N_{\text{tau}} + \beta N_{\text{bkg}}, \tag{1}$$

$$\chi^2 = \sum_{i=1}^{10} \frac{(N_i^{\text{obs}} - \alpha N_i^{\text{tau}} - \beta N_i^{\text{bkg}})^2}{\sigma_i^2}, \tag{2}$$

where N_i^{obs} is the number of the observed events, N_i^{tau} is the number of predicted tau neutrino events, N_i^{bkg} is the MC predicted number of atmospheric neutrino background events, and σ_i is the statistical error for the ith bin. The sample normalizations, α and β, are allowed to vary freely, and the zenith angle distribution is divided into 10 bins, from -1 to 1 [$\cos\theta = -1$ ($\cos\theta = 1$) refers to upward-going (downward-going) events]. The results of the fit are shown in Fig. 3.

The minimum χ^2 for the likelihood fit (the NN fit) is $\chi^2_{\text{min}} = 7.6/8$ DOF (9.8/8 DOF), and the χ^2 assuming no tau neutrino appearance is 16.3/9 DOF (18.2/9 DOF). The normalizations of the best fit for the likelihood fit (the NN fit) are $\alpha = 1.76$ (1.71) and $\beta = 0.90$ (0.99). After correcting for efficiencies, these correspond to a best fit tau neutrino appearance signal of 138 ± 48(stat) [134 ± 48(stat)] for the likelihood analysis (the NN analysis). As can be seen in Fig. 3, an excess of tau neutrino signals is observed in the upward-going direction, and the data distribution agrees better with the prediction including tau neutrino appearance estimated by MC simulation. The backgrounds that remain after applying all of the ν_τ event selection criteria are mostly deep-inelastic scattering (CC DIS: 61.4%; NC DIS: 27.1%).

Approximately $82.9 \pm 3.0\%$ of events are in common to the tau-enriched samples selected by both analyses, for which our MC simulation predicts 83.1% of events overlap. The results for the likelihood and the neural network analyses are consistent.

The systematic errors from Super-K atmospheric neutrino oscillation analysis are reevaluated for the present analysis; however, in this estimation, the uncertainty in the absolute normalization is assumed to be 20%. All error terms except for those affecting sub-GeV, PC, and upward-

TABLE II. Summary of systematic uncertainties for the expected number of ν_τ events (top) and for the observed number of ν_τ events (bottom). The best fit values for each error term are listed for both likelihood (LH) and neural network (NN) analyses.

Systematic uncertainties for expected ν_τ	LH (%)	NN (%)
Super-K atmospheric ν oscillation analysis (23 error terms)	21.6	20.2
Tau related:		
Tau neutrino cross section	25.0	25.0
Tau lepton polarization	7.2	11.8
Tau neutrino selection efficiency	0.4	0.5
LH selection efficiency	4.8	
NN selection efficiency		3.0
Total:	32.6	34.4

Systematic uncertainties for observed ν_τ	LH (%)	NN (%)
Super-K atmospheric ν oscillation analysis:		
Flux up/down ratio	6.5	5.7
Flux horizontal/vertical ratio	3.6	3.2
Flux K/π ratio	2.4	2.8
NC/CC ratio	4.3	3.8
Up/down asymmetry from energy calibration	1.4	<0.1
Oscillation parameters:		
$0.0020 < \Delta m^2_{23} < 0.0027$ eV^2	$+5.8$	$+8.8$
	-2.6	-3.3
$0.93 < \sin^2 2\theta_{23} < 1.00$	-3.3	-3.9
$0.0 < \sin^2 2\theta_{13} < 0.15$	-20.6	-17.9
Total:	$+10.7$	$+12.0$
	-22.9	-20.3

going muon events are considered. A detailed description of these uncertainties can be found in Ref. [7]. In addition, the uncertainties related only to the present analysis such as the ν_τ cross section, ν_τ polarization, tau likelihood, etc., are considered. The systematic uncertainties for the expected number of ν_τ events are summarized in Table II.

In determining the systematic uncertainties for the observed number of ν_τ events, various effects (such as up/down ratio) that could change the up-down asymmetry of the background MC events and the data are considered. The systematic errors due to uncertainties in the oscillation parameters, Δm^2_{23} and $\sin^2 2\theta_{23}$, are also estimated by using 68% C.L. allowed parameter region obtained by the L/E analysis from Super-K [6]. The uncertainty due to knowledge of the $\sin^2 2\theta_{13}$ is estimated using the limit obtained by the CHOOZ reactor neutrino experiment [16]. This systematic error is asymmetric because Multi-GeV electrons are expected to appear in the upward-going directions for nonzero θ_{13}, which would be backgrounds for ν_τ signals. Table II shows the summary of systematic uncertainties. We also performed a study to check dependency on Monte Carlo neutrino interaction models using another model, NUANCE [17]. The difference in the results is negligible.

Combining these errors with the fit result, we obtain a best fit tau neutrino appearance signal of $138 \pm 48(\text{stat})^{+15}_{-32}(\text{syst})$ from the likelihood analysis, which disfavors the no tau neutrino appearance hypothesis by 2.4 sigma. This is consistent with the expected number of tau neutrino events, $78 \pm 26(\text{syst})$ for $\Delta m^2 = 2.4 \times 10^{-3}$ eV^2, assuming the full mixing in $\nu_\mu \leftrightarrow \nu_\tau$ oscillations.

In conclusion, the search for the appearance of tau neutrinos from $\nu_\mu \leftrightarrow \nu_\tau$ oscillations in the atmospheric neutrinos has been carried out using atmospheric neutrino data observed in Super-Kamiokande-I. The tau neutrino excess events have been observed in the upward-going direction as expected. The Super-Kamiokande-I atmospheric neutrino data are consistent with $\nu_\mu \leftrightarrow \nu_\tau$ oscillations.

We gratefully acknowledge the cooperation of the Kamioka Mining and Smelting Company. The Super-Kamiokande experiment has been built and operated from funding by the Japanese Ministry of Education, Culture, Sports, Science and Technology, the United States Department of Energy, and the U.S. National Science Foundation.

[1] Y. Fukuda *et al.* (Super-Kamiokande Collaboration), Phys. Rev. Lett. **81**, 1562 (1998).
[2] Y. Fukuda *et al.* (Kamiokande Collaboration), Phys. Lett. B **335**, 237 (1994).

[3] M. Ambrosio *et al.* (MACRO Collaboration), Eur. Phys. J. C **36**, 323 (2004).
[4] W. W. M. Allison *et al.* (Soudan-2 Collaboration), Phys. Rev. D **72**, 052005 (2005).
[5] P. Adamson *et al.* (MINOS Collaboration), Phys. Rev. D **73**, 072002 (2006).
[6] Y. Ashie *et al.* (Super-Kamiokande Collaboration), Phys. Rev. Lett. **93**, 101801 (2004).
[7] Y. Ashie *et al.* (Super-Kamiokande Collaboration), Phys. Rev. D **71**, 112005 (2005).
[8] S. Fukuda *et al.* (Super-Kamiokande Collaboration), Phys. Rev. Lett. **85**, 3999 (2000).
[9] Y. Fukuda *et al.*, Nucl. Instrum. Methods Phys. Res., Sect. A **501**, 418 (2003).
[10] Y. Hayato, Nucl. Phys. B, Proc. Suppl. **112**, 171 (2002).
[11] S. Jadach, Z. Was, R. Decker, and J. H. Kuhn, Comput. Phys. Commun. **76**, 361 (1993).
[12] K. Hagiwara, K. Mawatari, and H. Yokoya, Nucl. Phys. **B668**, 364 (2003).
[13] J. D. Bjorken and S. J. Brodsky, Phys. Rev. D **1**, 1416 (1970).
[14] G. Hanson *et al.*, Phys. Rev. Lett. **35**, 1609 (1975).
[15] B. Schwindling, J. Mansouli'e, and O. Couet, MLPfit, http://schwind.web.cern.ch/schwind/MLPfit.html, 2000.
[16] M. Apollonio *et al.*, Eur. Phys. J. C **27**, 331 (2003).
[17] D. Casper, Nucl. Phys. B, Proc. Suppl. **112**, 161 (2002).